Non-proximity resonant tunneling in multi-core photonic band gap fibers: An efficient mechanism for engineering highly-selective ultra-narrow band pass splitters

Nikolaos. J. Florous, Kunimasa Saitoh, Tadashi Murao, and Masanori Koshiba

Division of Media and Network Technologies, Hokkaido University, Sapporo 060-0814, Japan
nflorous@dpo7.ice.eng.hokudai.ac.jp; ksaitoh@ist.hokudai.ac.jp; murao@icp.ist.hokudai.ac.jp; koshiba@ist.hokudai.ac.jp

Maksim Skorobogatiy

École Polytechnique de Montréal, Génie Physique,
C.P. 6079, succ. Centre-Ville Montreal, Québec H3C3A7, Canada
Maksim.skorobogatiy@polymt.ca

Abstract: The objective of the present investigation is to demonstrate the possibility of designing compact ultra-narrow band-pass filters based on the phenomenon of non-proximity resonant tunneling in multi-core photonic band gap fibers (PBGFs). The proposed PBGF consists of three identical air-cores separated by two defected air-holes which act as highly-selective resonators. With a fine adjustment of the design parameters associated with the resonant-air-holes, phase matching at two distinct wavelengths can be achieved, thus enabling very narrow-band resonant directional coupling between the input and the two output cores. The validation of the proposed design is ensured with an accurate PBGF analysis based on finite element modal and beam propagation algorithms. Typical characteristics of the proposed device over a single polarization are: reasonable short coupling length of 2.7 mm, dual bandpass transmission response at wavelengths of 1.339 and 1.357 μm, with corresponding full width at half maximum bandwidths of 1.2 nm and 1.1 nm respectively, and a relatively high transmission of 95% at the exact resonance wavelengths. The proposed ultra-narrow band-pass filter can be employed in various applications such as all-fiber bandpass/bandstop filtering and resonant sensors.

OCIS codes: (060.2430) Fibers, single mode; (999.9999) Photonic crystal fiber

References and links

1. P.St.J. Russell, "Photonic crystal fibers," Science **299**, 358-362 (2003).
2. S. Kawanishi, T. Yamamoto, H. Kubota, M. Tanaka, and S. Yamaguchi, "Dispersion controlled and polarization maintaining photonic crystal fibers for high performance network systems," IEICE Trans. Electron. **E87-C**, 336-342 (2004).
3. B.J. Mangan, J.C. Knight, T.A. Birks, P.St.J. Russell, and A.H. Greenaway, "Experimental study of dual-core photonic crystal fibre," Electron. Lett. **36**, 1358-1359 (2000).
4. W.N. MacPherson, J.D.C. Jones, B.J. Mangan, J.C. Knight, and P.St.J. Russell, "Two-core photonic crystal fiber for Doppler difference velocimetry," Opt. Commun. **233**, 375-380 (2003).
5. K. Kitayama and Y. Ishida, "Wavelength-selective coupling of two-core optical fiber: application and design," J. Opt. Soc. Am. A **2**, 90-94 (1985).
6. R. Zengerle and O.G. Leminger, "Narrow-band wavelength-selective directional couplers made of dissimilar single-mode fibers," J. Lightwave Technol. **LT-5**, 1196-1198 (1987).
7. E. Eisenmann and E. Weidel, "Single-mode fused biconical couplers for wavelength division multiplexing with channel spacing between 100-300 nm," J. Lightwave Technol. **LT-6**, 113-119 (1988).

8. K. Thyagarajan, S.D. Seshadri, and A.K. Ghatak, "Waveguide polarizer based on resonant tunneling," J. Lightwave Technol. **9**, 315-317 (1991).
9. K. Saitoh, N. Florous, M. Koshiba, and M. Skorobogatiy, "Design of narrow band-pass filters based on the resonant-tunneling phenomenon in multi-core photonic crystal fibers," Opt. Express **13**, 10327-10335 (2005). http://www.opticsinfobase.org/abstract.cfm?URI=oe-13-25-10327
10. M. Skorobogatiy, K. Saitoh, and M. Koshiba, "Transverse light guides in microstructured optical fibers," Opt. Lett. **31**, 314-316 (2006).
11. K. Saitoh and M. Koshiba, "Full-vectorial imaginary-distance beam propagation method based on a finite element scheme: application to photonic crystal fibers," IEEE J. Quantum Electron. **38**, 927-933 (2002).
12. K. Saitoh and M. Koshiba, "Full-vectorial finite element beam propagation method with perfectly matched layers for anisotropic optical waveguides," J. Lightwave Technol. **19**, 405-413 (2001).
13. K. Saitoh and M. Koshiba, "Leakage loss and group velocity dispersion in air-core photonic bandgap fibers," Opt. Express **11**, 3100-3109 (2003). http://www.opticsinfobase.org/abstract.cfm?URI=oe-11-23-3100
14. N. Florous, K. Saitoh, and M. Koshiba, "A novel approach for designing photonic crystal fiber splitters with polarization-independent propagation characteristics," Opt. Express **13**, 7365-7373 (2005). http://www.opticsinfobase.org/abstract.cfm?URI=oe-13-19-7365
15. S. K. Varshney, N. Florous, K. Saitoh, and M. Koshiba, "The impact of elliptical deformations for optimizing the performance of dual-core fluorine-doped photonic crystal fiber couplers," Opt. Express **14**, 1982-1995 (2006). http://www.opticsinfobase.org/abstract.cfm?URI=oe-13-19-7365
16. T. Tjugiarto, G.D. Peng, and P.L. Chu, "Bandpass filtering effect in tapered asymmetrical twin-core optical fibers," Electron. Lett. **29**, 1077-1078 (1993).
17. B. Wu and P.L. Chu, "Narrow-bandpass filter with gain by use of twin-core rare-earth-doped fiber," Opt. Lett. **18**, 1913-1915 (1993).
18. B. Ortega and L. Dong, "Accurate tuning of mismatched twin-core fiber filters," Opt. Lett. **23**, 1277-1279 (1998).

1. Introduction

In the last decade, photonic crystal fibers (PCFs) [1], also known as microstructured optical fibers (MOFs) or holey fibers have witnessed an unpredictable attention due to the fact that they can provide unprecedented degrees of freedom in engineering their modal characteristics. Although PCFs are usually formed by a central defect region surrounded by multiple air-holes arranged in a regular triangular lattice, recent advancements in manufacturing technology of PCFs such as multiple-capillary drawing method [2] can readily realize multi-core PCFs [3], [4].

An important element in all-optical fiber communication systems and all-optical fiber measurements is apparently a wavelength-selective fiber device such as a fiber filter. A number of fabrication techniques have been used so far for realizing such devices [5]-[7]. The operational principle of conventional fiber filters typically involves in transferring energy over a coupling length between two distinct fiber cores coupled by proximity interaction. However in this case modes in closely separated individual cores are phase-matched at all wavelengths, thus making it difficult to engineer bandpass filtering characteristics. It was recently shown that efficient band pass filters can be realized based on the resonant tunneling phenomenon [8] in multicore PCFs [9].

One of the major trends in the development of all-fiber devices is the increasing number of functionalities in a single fiber. The ultimate goal is to be able to fabricate in a single draw a complete all-fiber component provisioned on a preform level. Some of the advantages of all-fiber devices are: simplified packaging, absence of sub-component splicing losses, environmental stability due to the absence of free space optics. While the benefits of integrated all-fiber devices are significant enough to encourage development of increasingly complex components, the major roadblock to their realization is an unavoidable complexity of the required transverse refractive index profile. These challenges can be in a certain degree met by using a novel class of microstructured optical fiber coupler that was recently introduced in Ref. [10], which operates by resonant rather than proximity coupling, where energy transfer is realized via transverse lightguides integrated into the fiber's cross-section. Such a design allows unlimited spatial separation between interacting fibers which in turn,

eliminates inter-core crosstalk via proximity coupling. Controllable energy transfer between fiber cores is then achieved on highly directional transmission through transverse lightguides. The main advantage of this coupling mechanism is its inherent scalability as additional fiber cores could be integrated into the existing fiber cross-section simply by placing them far enough from the existing circuitry to avoid proximity crosstalk, and then making the necessary inter-core connections with transverse light "wires" in a direct analogy to the "on chip electronics integration".

Based on the above mentioned benefits that the resonant coupling mechanism can introduce, we devote the present paper to describe a novel design approach for realizing resonant bandpass filters in multicore photonic band gap fibers (MC-PBGFs) based on the highly-selective resonant tunneling mechanism. The MC-PBGF consists of three identical air-cores separated by two defected air-holes (resonators). By adjusting the sizes of the resonant air-holes, phase-matching at two distinct wavelengths can be achieved between the input and output cores, enabling highly-selective narrowband resonant directional coupling. Although other mature technologies such as fiber Bragg gating (FBG) with circulator have been successfully used to realize narrow-band filters, perhaps one of the appealing properties of the technology of multicore PBGFs is the exhibition of temperature and strain insensitivity in comparison to FBGs. Through an efficient modal [11] and beam propagation analysis [12], based on the finite element method (FEM), we theoretically investigate the possibility of synthesizing efficient ultra narrow-band splitters, suitable for filtering applications.

The composition of the present investigation will be as follows: in Section 2 we introduce the device concept and we give exact design guidelines for achieving the narrow bandpass filtering characteristics. Then in Section 3 we validate our design's performance by showing various numerical simulations based on FEM numerical algorithms. In Section 4 we briefly address the possibility of realizing a polarization-independent splitter operating at a single wavelength, based on the prescribed MC-PBGF technology. A final conclusion will follow in Section 5 with some suggestions for future investigations.

2. Schematic representation and design guidelines for engineering MC-PBGF splitters

The cross-section of the structure under investigation is shown in Fig. 1. The hollow cores are formed in a silica-based MOF with a cladding refractive index n = 1.45, by removing two rows of tubes and smoothing the resulting core edges. The pitch constant is chosen to be $\Lambda = 2$ μm, while the air-hole diameters in the cladding of the fiber is d/Λ=0.9, with a total of six hole layers in the cladding. Fundamental band gap where the core guided modes are found, extends between 1.29 μm < λ < 1.40 μm [13]. The formation of a splitter, operating at two distinct wavelengths, can be achieved by placing three hollow cores of N=5 periods apart from each other (along the x axis) as shown in Fig. 1. Two dissimilar transverse resonators with d_1/Λ and d_2/Λ are then introduced by reducing (high index defects) the diameters of the air-holes in the middle of the line joining the cores. By an accurate modal analysis performed using an accurate FEM solver [11], in Fig. 2 (a) we evaluate the effective indexes of the x-polarized (horizontally polarized) fundamental (blue solid curve), as well as the x-polarized excited resonant modes (red dashed curves), as a function of the operating wavelength and for several incremental values of the resonator's normalized diameter d_r/Λ, ranged from 0.6 to 0.8. Notice that the computation of the effective refractive index of the fundamental mode was performed assuming the core to be isolated; while the resonant excited modes have been calculated assuming these resonators isolated from the cores. This approximation was confirmed to give accurate results when comparing with the results associated with the coupled system's performance (cores plus resonators). We can clearly see that the effective index of the fundamental mode is being crossed at certain wavelengths by the excited resonant modes. The physical interpretation of this crossing is that the excited modes at wavelengths of λ_1, λ_2, λ_3, … , λ_n, corresponding to different normalized resonator's diameters d_r/Λ, can be effectively

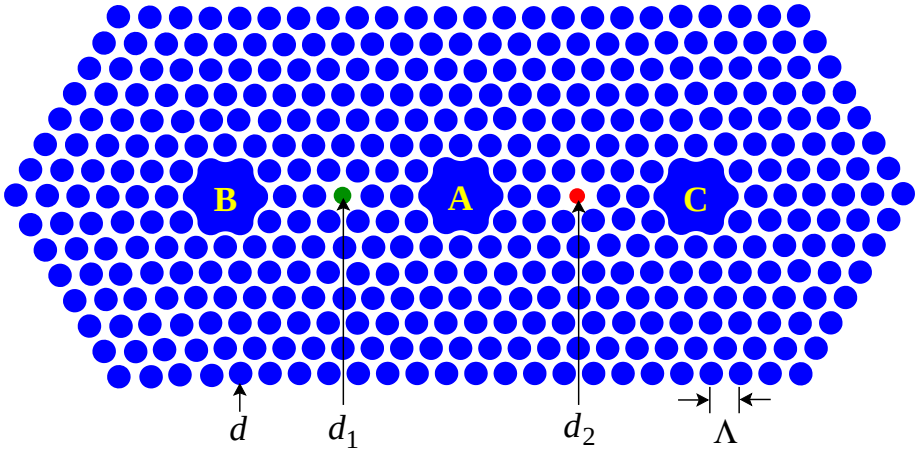

Fig. 1. Topology of a three-core PBG fiber splitter utilizing a non-proximity resonant tunneling coupling mechanism. The air-holes in the cladding are arranged in a triangular configuration with pitch constant Λ and air-hole diameters d. As an input core we consider the middle core-A, while B and C are the output cores. Two dissimilar transverse resonators with diameters d_1 (green colored) and d_2 (red colored) are then introduced by reducing (high index defects) the diameters of the air-holes in the middle of the line joining the cores. By a judicious choice of the design parameters this multicore PBGF can act as an ultra-narrow dual bandpass filter at a very short coupling length.

transferred via resonant coupling through the dissimilar resonators, from the central input core-A into the output cores-B and C. This simply means that at a given normalized resonator's diameter d_r/Λ, there exists a wavelength where resonant tunneling can be achieved between the input (core-A) and output (cores B or C) through the resonator. To identify the evolution of the resonance wavelengths as the resonator's diameter changes, in Fig. 2(b) we plot the resonance wavelength as a function of the resonator's normalized diameter d_r/Λ. From the results in Fig. 2(b) we can observe that as soon as the resonator's diameter decreases the resonance wavelength increases. Due to the fact that the resonance wavelength must lie within the PBG region (shown by the grey boundaries), the possible values of the resonator's diameters are in the range: $0.62 < d_r/\Lambda < 0.8$, for the x-polarized state. The same calculations are repeated in Figs. 3(a) and (b) for the y-polarization state (vertically polarized state). In the second case of y-polarization, we can observe a significant difference in the behavior of the evolution curve of the resonance wavelengths. By comparing the results in Figs. 2(b) and 3(b) we can see a great difference between the two polarizations. From Fig. 3(b) it is evident that the range of allowable values of the normalized resonator's diameters for the y-polarized mode which will result in resonance wavelengths within the PBG of the structure is significantly larger: $0 < d_r/\Lambda < 0.86$. In addition a very interesting phenomenon occurs. This phenomenon is the insensitivity of the resonance wavelength for the following range of the normalized resonator's diameters $0.1 < d_r/\Lambda < 0.4$, since at this range the resonance wavelength appears almost constant at a value of $\lambda_{res} = 1.372$ μm. The physical explanation for this drastic difference among the two polarization states can be given in terms of the feature of each polarization. This means that while the y-polarization has an even-type profile, the x-polarization significantly differs because its profile is anti-symmetric (odd), as will be demonstrated qualitatively later on. Therefore as a conclusion of this section we have described the basic principle of operation for this type of multi-core PBGF splitter and we have identified the impact of each polarization state to the resonance wavelength of the coupled system consisting of the input core and the resonator. In addition we have identified the allowable range that the resonators can give a resonance wavelength within the PBG capabilities of the structure.

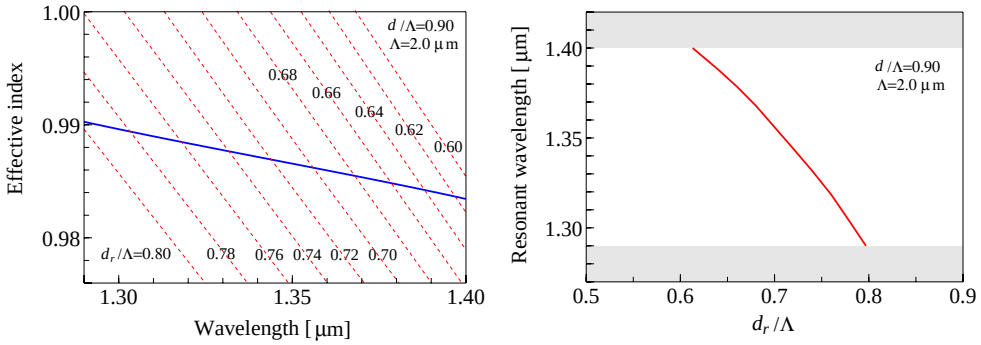

Fig. 2. (a) Effective indexes of the *x*-polarized fundamental (solid blue curve) and the *x*-polarized excited resonant modes (red dashed curves) of the multi-core PBG fiber splitter, for fixed design parameters d/Λ= 0.9, Λ= 2 μm, and for several values of the normalized resonator's diameter d_r/Λ, ranged from 0.6 to 0.8, and (b) the evolution of the resonance wavelength as a function of the resonator's normalized diameter d_r/Λ. In this case the requirement that the resonance wavelength must lie within the PBG of the structure (between the grey boundaries), limits the normalized resonator's diameter d_r/Λ to vary from 0.62 up to 0.8.

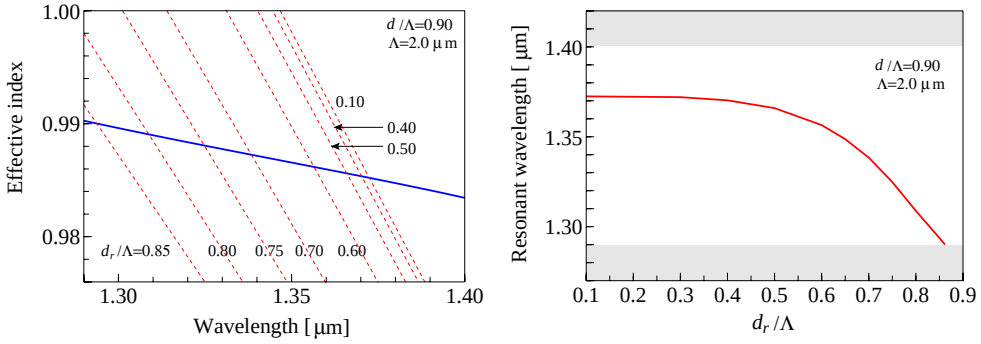

Fig. 3. (a) Effective indexes of the *y*-polarized fundamental (solid blue curve) and the *y*-polarized excited resonant modes (red dashed curves) of the multi-core PBG fiber splitter, for fixed design parameters d/Λ= 0.9, Λ= 2 μm, and for several values of the normalized resonator's diameter d_r/Λ, ranged from 0.1 to 0.85, and (b) the evolution of the resonance wavelength as a function of the resonator's normalized diameter d_r/Λ. Notice the remarkable insensitivity in the evolution of the resonant wavelength as a function of the resonator's diameter in the range from 0.1 to 0.4 for the *y*-polarization. The PBG boundary is denoted within the grey strips.

3. Numerical results and device performance

After having explained the basic operational principle of the device under consideration, we proceed by investigating the spectral as well as its propagation characteristics. The operational principle of this bandpass filter can be alternatively understood in terms of the supermodes of the "three-core" directional splitter (that is the system composed of two air-cores and one resonator). If the individual cores of the splitter are single-moded, the coupler structure supports three supermodes, two symmetric and one anti-symmetric (for *y*-polarization), and

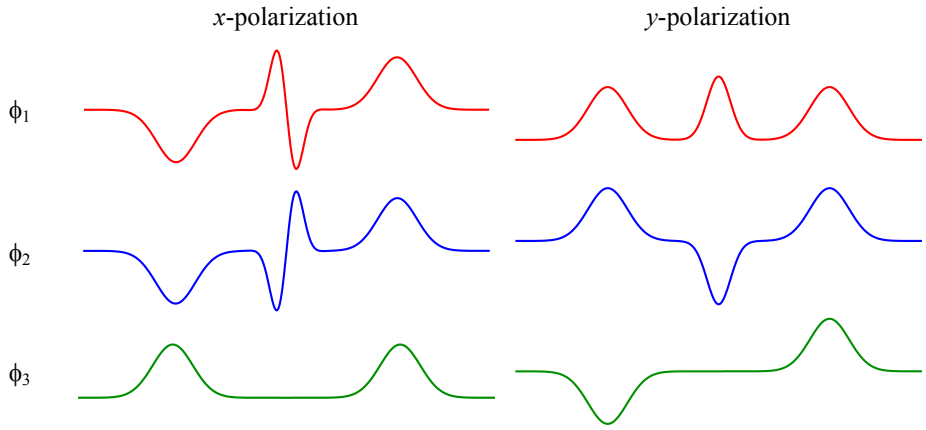

Fig. 4. Qualitative representation of the 3 supermodes existing in the MC-PBGF splitter.

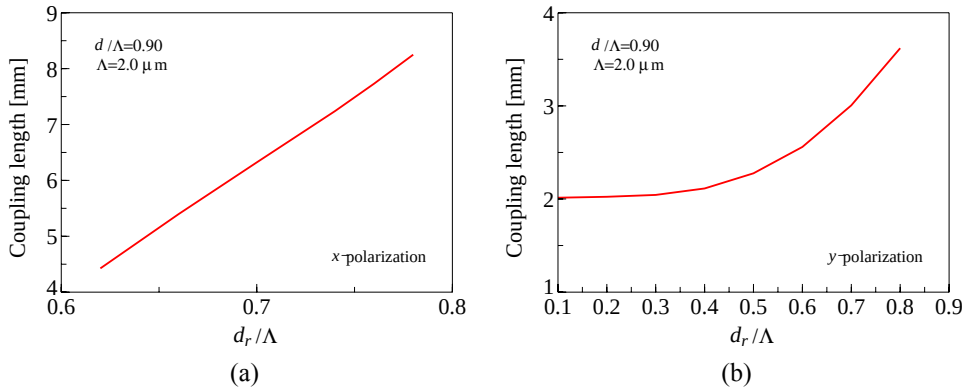

Fig. 5. Coupling length (mm) as a function of the normalized resonator's diameter d_r/Λ, for (a) *x*-polarization and (b) *y*-polarization. Observe the remarkable linear evolution of the curve in the case of *x*-polarization and the asymptotic behavior as the normalized diameter tends to lower values, for the *y*-polarization.

two anti-symmetric and one symmetric (for *x*-polarization), with corresponding fields defined as ϕ_1, ϕ_2, ϕ_3 and qualitatively shown in Fig. 4.

Let $n_{eff,1}$, $n_{eff,2}$, and $n_{eff,3}$ represent the effective refractive indices of the supermodes corresponding to the fields ϕ_1, ϕ_2, ϕ_3, respectively, for each of the polarization states. Then assuming that initially all the energy is in the input core-A, this will correspond to the excitation of a supermode combination of the following type:

$$\phi(z=0) = (\phi_1 + \phi_2)/2 + \phi_3 . \tag{1}$$

After propagation over a distance-*z*, this excitation pattern will evolve into:

$$\phi(z) = (\phi_1 \exp(-j\beta_1 z) + \phi_2 \exp(-j\beta_2 z))/2 + \phi_3 \exp(-j\beta_3 z) \tag{2}$$

where $\beta_i = 2\pi n_{eff,i}/\lambda_0$ (i = 1, 2, 3) and λ_0 is operating wavelength. If we design the PBGF so that the effective refractive indexes of its supermodes satisfy the condition:

$$n_{eff,1} - n_{eff,3} = n_{eff,3} - n_{eff,2} \tag{3}$$

or equivalently,

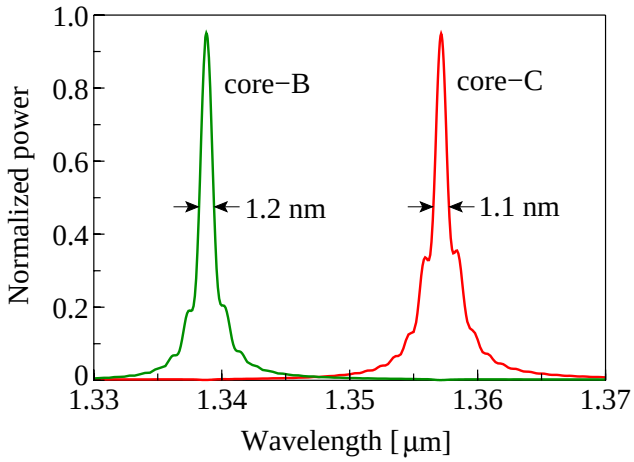

Fig. 6. Dual band-pass filtering characteristics for *y*-polarization of the three-core PBG fiber splitter, at the two resonant wavelengths of λ_1 = 1.339 μm and λ_2 = 1.357 μm, with corresponding full width at half maximum (FWHM) bandwidths of 1.2 nm and 1.1 nm, respectively. The transmission peak at the exact resonance wavelengths is about 95 % a result that indicates the slightly difference between the partial coupling lengths at the two different wavelengths.

$$2n_{eff,3} - n_{eff,1} - n_{eff,2} = 0 \quad , \tag{4}$$

complete power transfer from core A to core B or C can be achieved at the exact resonant wavelength λ_0 by choosing mode propagation length $z=L_c$ with

$$L_c^{x,y} = \frac{\lambda_0}{2(n_{eff,1}^{x,y} - n_{eff,3}^{x,y})} \tag{5}$$

where $n_{eff,1}^{x,y}$ and $n_{eff,3}^{x,y}$ denote the effective indexes of the supermodes, for *x*-polarization or *y*-polarization respectively. Assuming the following geometrical parameters of the PBGF for the *y*-polarized state: Λ = 2 μm, d/Λ=0.9, d_1/Λ=0.7 and d_2/Λ=0.6, from the results in Fig. 3(a) we can clearly see that the excited resonant modes crosses the effective index curve of the fundamental mode, at two distinct wavelengths of $\lambda_{1,y}$ = 1.339 μm and $\lambda_{2,y}$ = 1.357 μm. In case of *x*-polarization, by choosing the resonators sizes to be d_1/Λ=0.74 and d_2/Λ=0.70, the resonant wavelengths will be different: $\lambda_{1,x}$ = 1.331 μm and $\lambda_{2,x}$ = 1.356 μm. Using the relation in Eq. (5) combined with an accurate modal solver based on the FEM computational algorithm, in Fig. 5 we plot the calculated coupling lengths as a function of the normalized resonator's diameter d_r/Λ for (a) *x*-polarization and (b) *y*-polarization, respectively. From the results in Fig. 5 we can at first observe a significant difference of the coupling lengths evolution for the two different polarization states. Particularly from Fig. 5(a) we can see that the coupling length changes linearly as the resonator's diameter increases, while a different rate of change occurs in Fig. 5(b), where we can clearly see the asymptotic behavior of the coupling length as the resonator's diameter approaches lower values. The partial coupling lengths in this case are: $L_c^x(\lambda_1 = 1.331\ \mu m) = 7.3$ mm, $L_c^x(\lambda_2 = 1.356\ \mu m) = 6.4$ mm, $L_c^y(\lambda_1 = 1.339\ \mu m) = 2.9$ mm, and $L_c^y(\lambda_2 = 1.357\ \mu m) = 2.6$ mm. In Fig. 6 we plot the obtained spectral characteristics of this novel type of PBGF splitter with total fiber length of 2.7 mm, for the *y*-polarized state, by using an accurate analysis based on the BPM algorithm [12]. From these results we can observe a dual band-pass transmission response centered at the prescribed wavelengths of $\lambda_{1,y}$ = 1.339 μm and $\lambda_{2,y}$ = 1.357 μm. The highly selectivity in the

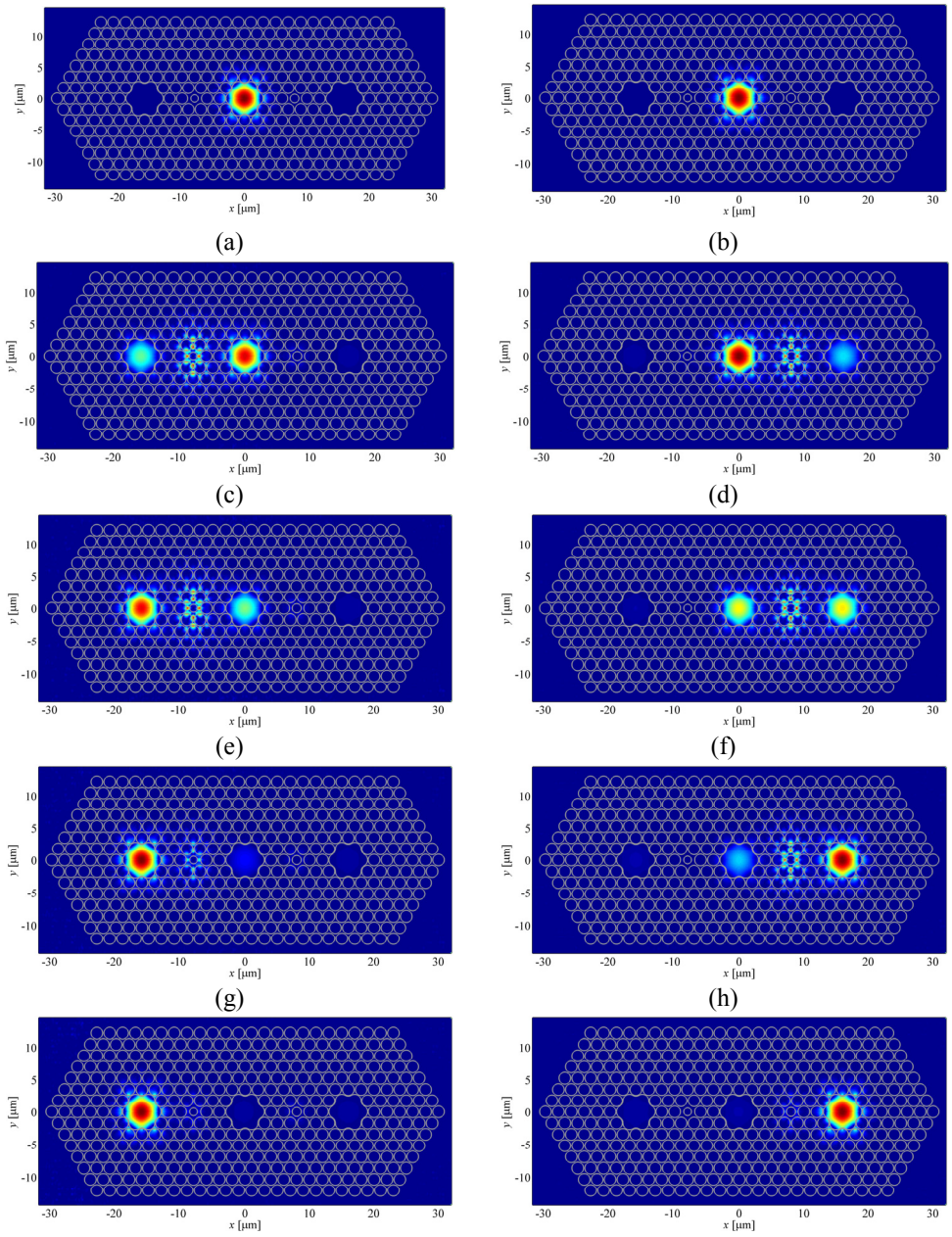

Fig. 7. Snapshots of the electric field distributions, that is *y*-polarization (E_y), in the multi-core PBGF splitter, for (a) $\lambda_{1,y}$ = 1.339 μm, (b) $\lambda_{2,y}$ = 1.357 μm, calculated at a distance of z = 0 mm, (c) $\lambda_{1,y}$ = 1.339 μm (d) $\lambda_{2,y}$ = 1.357 μm, at a distance of z = 1.0 mm, (e) $\lambda_{1,y}$ = 1.339 μm, and (f) $\lambda_{2,y}$ = 1.357 μm, at a distance of z = 1.5 mm, (g) $\lambda_{1,y}$ = 1.339 μm, and (h) $\lambda_{2,y}$ = 1.357 μm, at a distance of z = 2.0 mm, and finally for (i) $\lambda_{1,y}$ = 1.339 μm, (j) $\lambda_{2,y}$ = 1.357 μm, calculated at the coupling length of z=L_c= 2.7 mm. We can clearly see that at the coupling length of L_c= 2.7 mm, almost complete power transfer can be achieved from the input core-A to the output cores B and C at wavelengths of $\lambda_{1,y}$ = 1.339 μm and $\lambda_{2,y}$ = 1.357 μm, respectively with a transmission level of about 95 % due to the slightly difference in the values of the exact coupling lengths at the two different wavelengths.

filter's response we could obtain in this case, indicates the potential capability of the non-proximity resonator's states to synthesize highly selective resonant coupling characteristics. The full width at half maximum (FWHM) bandwidths of this filter are 1.2 nm and 1.1 nm for the *y*-polarized state at wavelengths of $\lambda_{1,y}$ = 1.339 μm and $\lambda_{2,y}$ = 1.357 μm, respectively, while for the *x*-polarized state the FWHM bandwidths were found to be a bit smaller. In both cases a transmission of about 95 % at the resonant wavelengths of λ_1 and λ_2 could be achieved. The difference in the values of the FWHM bandwidths for the two different polarization states, is associated with the larger coupling length of the *x*-polarization in comparison to the *y*-polarization (see Fig. 5), a fact which in general will result in a weaker coupling between the input core-A and the output cores-B or C for the *x*-polarization, thus resulting in a lower FWHM.

To visualize the power splitting mechanism in our proposed PBGF splitter, in Fig. 7 we plot the coupling characteristics of the field distribution at different propagation distances, obtained by using a BPM [12]. Specifically Fig. 7 shows the snapshots of the electric field distribution, that is *y*-polarized mode (E_y), for (a) $\lambda_{1,y}$ = 1.339 μm, (b) $\lambda_{2,y}$ = 1.357 μm, calculated at a distance of z = 0 mm, (c) $\lambda_{1,y}$ = 1.339 μm (d) $\lambda_{2,y}$ = 1.357 μm, at a distance of z = 1.0 mm, (e) $\lambda_{1,y}$ = 1.339 μm, and (f) $\lambda_{2,y}$ = 1.357 μm, at a distance of z = 1.5 mm, (g) $\lambda_{1,y}$ = 1.339 μm, and (h) $\lambda_{2,y}$ = 1.357 μm, at a distance of z = 2.0 mm, and finally for (i) $\lambda_{1,y}$ = 1.339 μm, (j) $\lambda_{2,y}$ = 1.357 μm, calculated at the coupling length of $z = L_c$ = 2.7 mm. We can clearly observe that at the coupling length of L_c = 2.7 mm the two different wavelengths were splitted in the output cores B and C within a power decrement of 5 % from the targeted level of 100 %, associated with the slightly difference between the partial coupling lengths corresponding to the two different operating wavelengths.

4. Realization of polarization-insensitive PBGF splitters operating at a single wavelength

In the previous sections we have devoted our efforts to design PBGF splitters operating at two distinct wavelengths and for two different polarization states. One of the main conclusions was that the selection of polarization is very important in terms of the device propagation characteristics. Recently there has been much effort in realizing polarization-independent splitters based on the PCF technology [14], [15]. In this section we will show that by using the prescribed multicore PBGF topology with an appropriate selection of the design parameters,

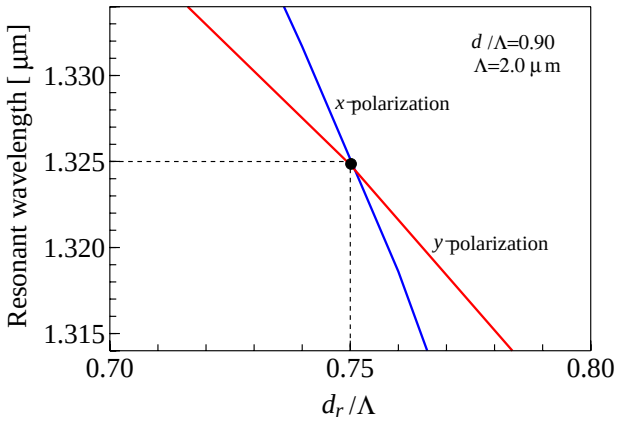

Fig. 8. Evolution of the resonance wavelengths, as a function of the resonator's normalized diameter d_r/Λ, for *x*-polarization (blue curve) and *y*-polarization (red curve). The two curves dissect at a point corresponding to resonance wavelength of λ_{res} = 1.325 μm and normalized resonator's diameter d_r/Λ= 0.75. Thus by fixing both resonators' diameters at the prescribed value, polarization-independent propagation characteristics can be realized at a single wavelength of λ_{res} = 1.325 μm.

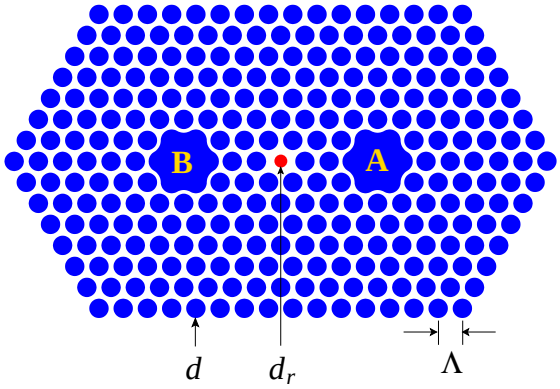

Fig. 9. Dual-core PBGF splitter with an embedded resonator in its profile, for achieving polarization-independent propagation characteristics.

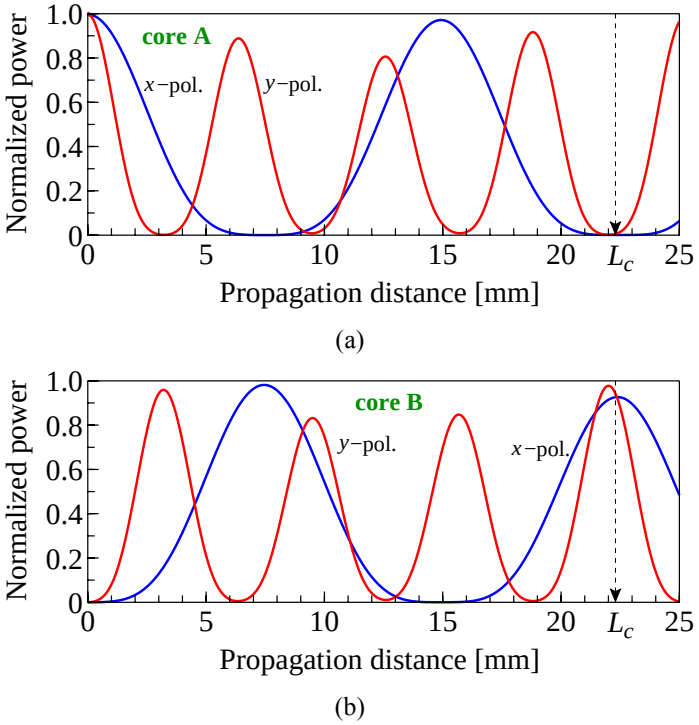

Fig. 10. Normalized power distribution in the MC-PBGF-splitter for *x*-polarization (blue curve), and *y*-polarization (red curve), at operating wavelength of λ_{res} = 1.325 μm, and for (a) input core-A, (b) output core-B. The coupling length for polarization-independent operation was confirmed by the BPM analysis to be L_c = 22.3 mm. Thus by fixing the MC-PBGF splitter's length at the prescribed value, the structure operates as a dual-core coupler, with a transmittivity of more than 90 %, independent of the polarization state.

polarization-independent propagation characteristics can be achieved at a single operational wavelength. We refer to the results obtained in Figs. 2(b) and 3(b), and we combine these results to generate Fig. 8, for the structure shown in Fig. 9, where we can see the evolution of the resonance wavelength curves as a function of the resonator's normalized diameter

d_r/Λ, for *x*-polarization (blue curve) and *y*-polarization (red curve). These two curves cross each other at a unique point corresponding to $d_r/\Lambda=0.75$ with resonance wavelength of $\lambda_{res} = 1.325$ μm. This unique selection of the resonator's diameter will lead to polarization-independent propagation characteristics, for the structure shown in Fig. 9, at the prescribed single resonance wavelength. So by choosing the resonator's diameter as $d_r/\Lambda=0.75$, the resulting structure will operate as an effectively 100 % coupler from core-A into core-B, with polarization-independent propagation characteristics, operating at a single wavelength. The corresponding coupling length in this case was calculated by the modal analysis to be L_c = 22.3 mm, a relatively short coupling length, acceptable for most practical applications. In order to verify the exact coupling length, in Fig. 10 we perform a simulation of the normalized power propagation along the PBGF splitter, using an accurate BPM algorithm [12]. Specifically Fig. 10 (a) shows the normalized power propagation at the resonance wavelength of $\lambda_{res} = 1.325$ μm, for *x*-polarization (blue curve), and *y*-polarization (red curve), in the input core-A as a function of the propagating distance in mm. The same simulation is shown in Fig. 10 (b) for the output core-B. From these results we can see that at the coupling length of L_c = 22.3 mm, the power is transferred from the input core-A to the output core-B with a transmission of more than 90 %, independent of the polarization state of the input signal. The main conclusion arising from this section is that the proposed MC-PBGF technology has indeed the potential capabilities of realizing polarization-independent devices by a judicious choice of the design parameters.

5. Conclusions

To summarize our work, we have proposed and numerically investigated the propagation properties of a novel bandpass filter based on the resonant tunneling phenomenon in a three-core PBGF. The design strategy of realizing multi-core couplers based on the resonant tunneling effect in PBGFs, according to the best of our knowledge, is reported in the international literature for the first time. Results of a full vectorial finite element modal analysis confirmed by BPM simulations have been presented for a variety of quantities related to the fiber's propagation characteristics. The high suppression of the side-lobes in comparison to previous reported filters based on conventional fiber technology [16]-[18] as well as the ultra-narrowband response and the reasonable short coupling length are the main advantages of the proposed PBGF architecture. Additionally we have showed that by using this MC-PBGF platform we can even achieve polarization-independent propagation characteristics at a single operational wavelength. Regarding the feasibility of our proposed fiber, maybe a little bit tedious at the present stage of technology, but we strongly believe that with more advanced fabrication technologies that will be introduced in the near future, the proposed MC-PBGF splitter will be a challenging fabrication task for the experimentalists. Our three-core PBGF coupler can be employed in multifunctional all-fiber bandpass/bandstop filtering applications.

A generalized wavelength splitter based on the resonant tunneling effect in multi-core PBGFs with multiple integrated resonators in its profile, is proposed for future analysis in Fig. 11. The operational principle is exactly the same as that of the splitter in Fig. 1. By an appropriate choice of the design parameters the generalized wavelength splitter in Fig. 11 can perform a four-wavelength splitting operation within reasonably short coupling length, appropriate for the realization of multi-operational all-fiber devices. We believe that the inclusion of multiple integrated components in a single fiber for multifunctional purposes is a challenging problem and currently is an active research topic in our group.

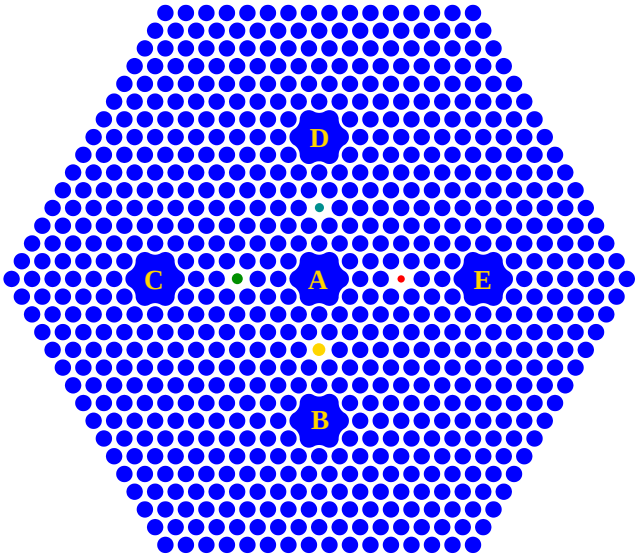

Fig. 11. Topology of the proposed five-core PBGF splitter utilizing a non-proximity resonant tunneling coupling mechanism. As an input core we consider the central core-A, while B, C, D and E are the output cores. Four dissimilar transverse resonators with diameters d_1 (yellow colored), d_2 (green colored), d_3 (teal colored), and d_4 (red colored) are introduced by reducing (high index defects) the diameters of the air-holes across the lines joining the cores. By a judicious choice of the design parameters this multicore PBGF can perform an ultra-narrow bandpass filtering operation at four distinct wavelengths with a reasonably short coupling length.

Acknowledgements

The authors would like to acknowledge partial financial support of this project from the Postdoctoral Fellowship Program of the Japan Society for the Promotion of Science (JSPS).